



Universiteit
Leiden
The Netherlands

White matter hyperintensity shape is associated with cognitive functioning: the SMART-MR study

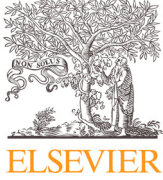
Zwartbol, M.H.T.; Ghaznawi, R.; Jaarsma-Coes, M.; Kuijf, H.; Hendrikse, J.; Bresser, J. de; ... ; UCC-SMART Study Grp

Citation

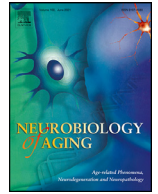
Zwartbol, M. H. T., Ghaznawi, R., Jaarsma-Coes, M., Kuijf, H., Hendrikse, J., Bresser, J. de, & Geerlings, M. I. (2022). White matter hyperintensity shape is associated with cognitive functioning: the SMART-MR study. *Neurobiology Of Aging*, 120, 81-87.
doi:10.1016/j.neurobiolaging.2022.08.009

Version: Publisher's Version
License: [Creative Commons CC BY 4.0 license](https://creativecommons.org/licenses/by/4.0/)
Downloaded from: <https://hdl.handle.net/1887/3567666>

Note: To cite this publication please use the final published version (if applicable).

Contents lists available at [ScienceDirect](https://www.sciencedirect.com)

Neurobiology of Aging

journal homepage: www.elsevier.com/locate/neuaging.org

White matter hyperintensity shape is associated with cognitive functioning – the SMART-MR study

Maarten H.T. Zwartbol^a, Rashid Ghaznawi^{a,b}, Myriam Jaarsma-Coes^{a,c}, Hugo Kuijff^d, Jeroen Hendrikse^a, Jeroen de Bresser^c, Mirjam I. Geerlings^{b,*}, on behalf of the UCC-SMART Study Group^e

^a Department of Radiology, University Medical Center Utrecht and Utrecht University, Utrecht, the Netherlands

^b Julius Center for Health Sciences and Primary Care, University Medical Center Utrecht and Utrecht University, Utrecht, the Netherlands

^c Department of Radiology, Leiden University Medical Center, Leiden, the Netherlands

^d Image Sciences Institute, University Medical Center Utrecht, Utrecht, the Netherlands

^e Listed in acknowledgements

ARTICLE INFO

Article history:

Received 13 December 2020

Revised 22 July 2022

Accepted 17 August 2022

Available online 23 August 2022

Keywords:

White matter hyperintensities

Cognitive functioning

SMART-MR study

Aging

MRI

Shape analysis

ABSTRACT

White matter hyperintensity (WMH) shape has been associated with the severity of the underlying brain pathology, suggesting it is a potential neuroimaging marker of WMH impact on brain function.

In 563 patients with vascular disease (58 ± 10 years), we examined the relationship between WMH volume, shape, and cognitive functioning. WMH volume and shape were automatically determined on 1.5T brain MRI data. Standardized linear regression analyses estimated the association between WMH volume and shape (concavity index, solidity, convexity, fractal dimension, and eccentricity) and memory and executive functioning, adjusted for age, sex, educational level, and reading ability.

Larger WMH volumes were associated with lower executive functioning Z-scores (b (95%-CI): -0.09 (-0.17 ; -0.01)). Increased shape complexity of periventricular/confluent WMH associated with lower executive functioning (concavity index $+1SD$: -0.13 (-0.20 ; -0.06); solidity $-1SD$: -0.09 (-0.17 ; -0.02)) and lower memory function (fractal dimension $+1SD$: -0.10 (-0.18 ; -0.02)). Of note, the association between concavity index and executive functioning was independent of WMH volume (-0.12 (-0.19 ; -0.04)).

Our results suggest that WMH shape contains additional information about WMH burden, not otherwise captured by WMH volume.

© 2022 The Author(s). Published by Elsevier Inc.

This is an open access article under the CC BY license (<http://creativecommons.org/licenses/by/4.0/>)

1. Introduction

White matter hyperintensities of presumed vascular origin (WMH) are a common finding in magnetic resonance imaging (MRI) of the aging brain and represent a key imaging feature of cerebral small vessel disease (CSVD) (Gouw et al., 2011; Wardlaw et al., 2013). CSVD comprises a group of neuropathological disease processes with various etiologic and pathologic correlates and neuroimaging features (Pantoni, 2010).

Previous studies have shown that increased WMH volume is associated with worse cognitive functioning, but the effect sizes

on individual cognitive domains are relatively small (Gouw et al., 2011; Vogels et al., 2007; Kloppenborg et al., 2014). An explanation for these small effect sizes could be that WMH volume is a relatively crude metric that does not fully capture the heterogeneity of the underlying pathology (Gouw et al., 2011). Histopathologic studies have shown that WMH shape is related to the underlying pathology, for example, smooth periventricular WMH are associated with mild, non-ischemic, parenchymal changes, whereas confluent and irregular WMH are associated with more severe changes, such as spongiosis and necrosis (Gouw et al., 2011). This suggests that, compared to volume, WMH shape may be a more important determinant of the functional consequences of WMH.

Recently, we showed that WMH shape can be automatically determined on magnetic resonance imaging (MRI) data (de Bresser et al., 2018; Ghaznawi et al., 2019). Furthermore, we showed that WMH shape is associated with different underlying etiology

* Corresponding author at: Julius Center for Health Sciences and Primary Care, University Medical Center Utrecht and Utrecht University, P.O. Box 85500, Stratenum 6.131, Utrecht, GA, 3508, the Netherlands Tel.: +31 887 550 670

E-mail address: m.geerlings@umcutrecht.nl (M.I. Geerlings).

(de Bresser et al., 2018), and that a more complex WMH shape is associated with presence of lacunes (Ghaznawi et al., 2019) and with physical frailty (Kant et al., 2019). Another study has shown that the irregularity of WMH was related to mental speed and fluid abilities, where in this study WMH volume was not (Lange et al., 2017). This suggests that WMH shape could show a better potential as a descriptor of the relation between WMH and certain cognitive functions (Lange et al., 2017). Therefore, in the current study we examined the relationship between WMH volume and shape and cognitive functioning in a large group of patients with vascular disease.

2. Material and methods

2.1. Study sample

The Second Manifestations of ARterial disease-Magnetic Resonance (SMART-MR) study is a prospective cohort study at the University Medical Center Utrecht with the objective to study determinants and clinical correlates of brain changes on MRI in patients with vascular disease (Geerlings et al., 2010). From May 2001 to December 2005, patients newly referred to the University Medical Center Utrecht with coronary artery disease, cerebrovascular disease, peripheral arterial disease, or an abdominal aortic aneurysm, and without MRI contraindications, were asked to participate. A total of 1309 patients were enrolled during this period. On a single visit to the University Medical Center Utrecht all patients underwent: a physical examination, carotid ultrasound, blood and urine samplings, and 1.5T brain MR imaging.

Questionnaires were used for the assessment of demographics, risk factors, medical history, medication use and cognitive and physical functioning. Neuropsychological assessment was introduced in the study in 2003 and performed on the same day as the other examinations.

For the current analysis, we had to exclude patients because of missing MRI data of one or more MRI sequences due to motion artifacts or logistic reasons ($n = 239$), irretrievable MRI data ($n = 19$), unreliable brain volume data due to motion artifacts in all three MRI sequences ($n = 44$), severe undersegmentation of WMH by the automated segmentation program ($n = 4$), and no WMH greater than five voxels ($n = 4$). Moreover, because of the later introduction of neuropsychological assessment during the enrollment period, data on cognitive functioning was not available in all patients, leaving 563 patients for the current study.

The SMART-MR study was approved by the medical ethics committee of the University Medical Center Utrecht according to the guidelines of the Declaration of Helsinki of 1975 and written informed consent was obtained from all patients.

2.2. Vascular risk factors

Questionnaires were used to assess smoking habits, alcohol intake, medication use and educational level. An overnight fasted venous blood sample was used to determine glucose and lipid levels. Height and weight were measured, and the body mass index (BMI) was calculated (kg/m^2). Systolic blood pressure (mmHg) and diastolic blood pressure (mmHg) were measured twice with a sphygmomanometer, and the averages of the two measures were calculated. Hypertension was defined as a mean systolic blood pressure of ≥ 160 mmHg, a mean diastolic blood pressure of ≥ 95 mmHg, self-reported use of antihypertensive drugs, or a known history of hypertension at inclusion. Diabetes mellitus was defined as use of glucose-lowering drugs, a history of diabetes mellitus, or a fasting plasma glucose level of > 11.1 mmol/L. Hyperlipidemia was defined as total cholesterol of > 5.0 mmol/L, a low-density lipopro-

tein cholesterol of > 3.2 mmol/L, use of lipid-lowering drugs, or a known history of hyperlipidemia.

2.3. Neuropsychological assessment

Neuropsychological tests were used to assess memory and executive functioning (Muller et al., 2011). Memory was assessed with the 15 Word Learning Test (a modification of the Rey Auditory Verbal Learning test) using a composite score of: the immediate recall based on 5 trials, the delayed recall, and the retention score; and the delayed recall of the Rey-Osterrieth Complex figure test (Brand and Jolles, 1985; Osterrieth P., 1944). Executive functioning was assessed with the Visual Elevator test, the Brixton Spatial Anticipation test, and the Verbal Fluency test using the letter *n* (Burgess and Shallice, 1996; Robertson et al., 1996; Wilkins et al., 1987). Natural logarithm transformation was applied to the Visual Elevator test scores, because of non-normal distribution. For the Visual Elevator test and the Brixton Spatial Anticipation test, scores were multiplied by -1 to ensure that lower scores represented worse performance. Lastly, composite domain-specific Z-scores were calculated. Reading ability, a measure of premorbid intellectual functioning, was assessed using the Dutch version of the National Adult Reading Test (Schmand et al., 1998). Educational level was divided into 7 categories: graded from primary school (around 6 years of education) to academic degree (around 16 years of education), according to the Dutch educational system.

2.4. Brain MRI

Brain MRI scans were performed on a 1.5 T whole-body system (Gyrosan ACS-NT, Philips Medical Systems, Best, The Netherlands). The standardized scan protocol consisted of four two-dimensional sequences (transversal acquisition, 38 contiguous slices, and $1.0 \times 1.0 \times 4.0$ mm³ voxel size): T1-weighted [repetition time (TR) = 235 ms; echo time (TE) = 2 ms], T1-weighted inversion recovery [TR = 2900 ms; TE = 22 ms; TI = 410 ms], T2-weighted [TR = 2200 ms; TE = 11 ms], and fluid-attenuated inversion recovery (FLAIR) images [TR = 6000 m; TE = 100 ms; inversion time (TI) = 2000 ms].

2.5. Image processing of brain volumes and WMH volume and type

A probabilistic segmentation method using *k*-nearest neighbor classification was used to segment gray matter, white matter, cerebrospinal fluid, and WMH (Anbeek et al., 2004) using the T1-weighted, FLAIR, and T1-weighted inversion recovery sequences of the MRI scans. Cerebral infarcts were manually segmented. Segmentation of WMH was checked by an investigator (RG) blinded to patient characteristics using an image processing framework (MeVisLab 2.7.1, MeVis Medical Solutions AG, Bremen, Germany), and corrected if needed.

Segmentation of the lateral ventricles was performed using the automated lateral ventricle delineation (ALVIN) algorithm in Statistical Parametric Mapping 8 (SPM8, Wellcome Trust Centre for Neuroimaging, University College London, London, UK) for Matlab (The MathWorks, Inc., Natick, MA, USA) (Ghaznawi et al., 2019; Kempton et al., 2013). The ALVIN mask was used to establish the margins of the lateral ventricles.

WMH probability data were processed into binary data using a threshold of 0.10. The arbitrary chosen threshold of 0.1 resulted in a good balance between retaining information and introduction of noise. A WMH lesion was defined as a group of voxels with touching corners, edges or faces. We labeled WMH lesions as periventricular, confluent or deep, based on their contiguity with

the ventricular margins and depth of extension into the white matter (Ghaznawi et al., 2019). Periventricular WMH were defined as lesions contiguous with the margins of the lateral ventricles and extending up to 10 mm from the lateral ventricles. Confluent WMH were defined as lesions contiguous with the margins of the lateral ventricles and extending more than 10 mm from the lateral ventricles. Deep WMH were defined as lesions that were not contiguous with the lateral ventricles (regardless of their distance to the ventricular margins). Labels were visually checked by an investigator (MJC) blinded to patient characteristics and corrected if needed.

Total periventricular, confluent and deep WMH volumes were obtained by summing all WMH lesion volumes per type. Total WMH volume was calculated by summing all WMH lesion volumes. Total brain volume was calculated by summing the volumes of gray matter, white matter, total WMH and other brain lesions. Intracranial volume was calculated by summing the cerebrospinal fluid volume and total brain volume (Geerlings et al., 2010).

2.6. Image processing of WMH shape

We analyzed WMH shape with the use of shape features (de Bresser et al., 2018). Shape features were calculated from the binary WMH segmentation data using Matlab.

The selection of WMH shape features has been described in detail in a prior study (Ghaznawi et al., 2019). In short, we first examined which shape features are able to describe the complexity of periventricular, confluent and deep WMHs (Ghaznawi et al., 2019). Next, the shape features were graded using the following criteria: comprehensibility (the ability to relate the shape feature output to the visual interpretation of WMH shape on MRI), usability on 1.5T MRI resolution, volume dependence (the degree to which a shape feature is correlated with WMH volume), robustness (the degree to which WMH positioning influences the shape feature), presence of a flooring effect (the minimum measured value is close to or similar to the smallest possible value of the shape feature) and presence of a ceiling effect (the maximum measured value is close to or similar to the highest possible value of the shape feature) (Ghaznawi et al., 2019). The shape features with the best combination of criteria (e.g., high comprehensibility, limited volume dependence, usability on 1.5T MRI data, adequate robustness, limited flooring and/or ceiling effect) were selected. The selected shape features and their definitions are presented in Supplemental Table 1. We decided to group the periventricular WMH and confluent WMH together into periventricular/confluent WMH. Although confluent WMH is a more heterogeneous group than periventricular WMH (because it contains periventricular WMHs which extend into the deep white matter but also deep WMH which extend into the periventricular white matter to the ventricular wall), they can be regarded as ends on the same spectrum (Fazekas 1/2 vs. Fazekas 3), are morphologically more similar (compared to deep WMH) and well-described by the same shape features.

We analyzed periventricular and confluent WMHs by calculating their convex hulls and obtaining volume and surface area ratios. Convexity was obtained by dividing the area of the convex hull by the WMH lesion's surface area. Solidity was calculated by dividing the volume of the WMH lesion by the volume of its hull. The concavity and solidity of a WMH lesion were used to calculate its concavity index (Liu et al., 2015).

We analyzed deep WMHs by dividing their minor axis by their major axis, which presents their eccentricity.

Lastly, fractal dimension was calculated for periventricular, confluent and deep WMHs. It was calculated with the box-counting method (Minkowski-Bouligand dimension) (Supplemental Table 1) as implemented in Matlab by Frederic Moisy (Moisy, 2008). We chose for box-counting because it is a straightforward and robust

method which can be applied easily to a large variety of shapes. The algorithm works as follows. As a general step, the binarized WHM image is partitioned into square boxes of size $r \times r \times r$ and the number of boxes ($n(r)$) containing a portion of the shape are counted. The algorithm starts with the smallest box fitting the entire binarized WMH and being a 2 multiple of the voxel size. Next, r is divided by two and the process repeated, each time dividing r by 2 until the voxel size is reached. The fractal dimension is calculated as the absolute value of the slope of the line obtained from the linear regression of the $(\log(n(r)), \log(1/r))$ curve. Visual examples of this calculation are shown in Supplemental Fig. 1. The images show an excellent correlation between the input data and the fitted linear regression, indicating that the FD computation is valid. In addition, the code was verified using an artificial 'Menger Sponge', which resulted in the expected value of 2.7. All shape values were expressed as mean values per patient with only fractal dimension having separate mean values per WHM subgroup (periventricular, confluent, and deep WMH).

The reproducibility of the WMH shape feature calculation was examined because of the potential influence of manual infarct segmentation. In a random dataset of 15 persons with infarcts a second rater repeated the process of automatic brain segmentation, manual infarct segmentation and WMH shape feature calculation. Spearman's ρ was used to test for correlations between the initial and second segmentations. With a correlation coefficient of 1.0 for each of the WMH shape features, the reproducibility of the shape feature calculation was regarded as excellent.

2.7. How to interpret WMH shape parameters

We use the term 'complexity' to denote roughness of a shape.

Solidity and convexity both measure roughness, solidity on a morphological level, and convexity on a textural level (Liu et al., 2015). As can be derived from Supplemental Table 1, lower solidity and convexity indicate a more complex shape. For example, a WMH with several long protrusions will likely have a relatively large convex hull volume compared to the contained WMH volume, which will cause solidity to trend downward.

Concavity index is a compound parameter that combines the information from solidity and convexity into a single parameter (Liu et al., 2015). As shown in Supplemental Table 1, a lower solidity and/or convexity will lead to a higher concavity index. Hence, a higher concavity index correlates with a more complex shape.

Fractal dimension is another measure of textural roughness and higher values indicate a more geometrically complex surface area of a WMH lesion (Esteban et al., 2009; Zhang et al., 2006).

Eccentricity measures the form of a shape (Loizou et al., 2015; Murphy et al., 2009). A lower eccentricity means a more elongated lesion, while a higher eccentricity means a relatively round WMH lesion. Of note, for convexity and solidity lower values indicate higher complexity whereas for concavity index and fractal dimension higher values indicate higher complexity. We have clarified this in the results section with the use of negative or positive standard deviations.

2.8. Statistical analysis

Baseline characteristics and WMH volume and shape features were calculated for the study sample.

Standardized linear regression analyses were used to estimate the association between total WMH volume Z-scores and WMH shape feature Z-scores with Z-scores of memory and executive functioning. WMH volume was natural-log transformed, to achieve a normal distribution, and expressed as a percentage of intracranial volume (%ICV), to adjust for variations in head size. All anal-

Table 1
Characteristics of the study sample (N=563)

Age (years)	58.1 ± 10.2
Sex, % male	76
Educational level (range 0 – 7)	3 (1 – 6)
Reading ability (range 0 – 100)	83 (56 – 97)
Alcohol use, % current	75
Cigarette smoking (pack-years)	18.2 (0.0; 50.4)
Hypertension, %	55
Diabetes, %	19
Hyperlipidemia, %	79
History of arterial disease	
Coronary heart disease, %	58
Cerebrovascular disease, %	20
Peripheral artery disease, %	25
Abdominal aortic aneurysm, %	8

Characteristics are presented as mean ± SD, % or median (10th, 90th percentile).

Table 2
WMH volume and shape features of the study sample (N=563)

WMH volume (mL)	
Total WMH	0.81 (0.17; 5.51)
Periventricular/confluent WMH	0.66 (0.12; 4.86)
Deep WMH	0.06 (0.01; 0.75)
Periventricular/confluent WMH shape features	
Solidity	0.63 (0.24; 0.91)
Convexity	1.03 (0.91; 1.28)
Concavity index	1.04 (0.94; 1.17)
Fractal dimension	1.22 (0.96; 1.51)
Deep WMH shape features	
Eccentricity	0.47 (0.30; 0.67)
Fractal dimension	1.44 (1.29; 1.63)

Values are median (10th; 90th percentile).

Key: WMH, white matter hyperintensities.

yses were adjusted for age, sex, level of education, and reading ability (model 1). The analyses of WMH shape features were additionally adjusted for natural-log transformed total WMH volume (%ICV) (model 2) to test if the associations were independent of WMH volume. The covariates were added on the basis of their known influence on cognitive functioning and/or for being a potential confounder. A *p*-value of < 0.05 was considered to be statistically significant. SPSS 25.0 for Windows (Chicago, IL, USA) was used to analyze the data.

3. Results

Characteristics of the 563 patients in our study sample (58 ± 10 years; 76% male) are presented in [Table 1](#). The total WMH volume and WMH shape features are shown in [Table 2](#). The median (10th; 90th percentile) total WMH volume was 0.81 mL (0.17; 5.51).

Larger total WMH volume Z-scores were associated with lower executive functioning Z-scores ($b = -0.09$; 95% CI -0.17 to -0.01) after adjusting for age, sex, educational level, and reading ability ([Table 3](#)). The adjusted R^2 of this model was 0.34. Larger total WMH volume Z-scores were also associated with lower memory Z-scores, but this association did not reach statistical significance ($b = -0.08$; 95% CI -0.16–0.00; $p = 0.06$).

A more complex shape of periventricular/confluent WMH was associated with lower executive functioning Z-scores (concavity index +1SD: $b = -0.13$; 95% CI -0.20 to -0.06; solidity -1SD: $b = -0.09$; 95% CI -0.17 to -0.02) after adjusting for age, sex, educational level, and reading ability ([Table 3](#)). After additional adjustment for total WMH volume, the association between concavity index and executive functioning remained significant (concavity index +1SD: $b = -0.12$; 95% CI -0.19 to -0.04), showing that this association was independent of WMH volume. The adjusted R^2 of the latter model

was 0.351 whereas the model without WMH volume adjustment had an adjusted R^2 of 0.350. This shows that WMH volume does not explain additional variation in executive functioning, compared to concavity index. Furthermore, it suggests that concavity index explains a little bit more variation in executive functioning compared to WMH volume alone, shown by the adjusted R^2 of 0.34. A more complex shape of periventricular/confluent WMH was also associated with lower memory Z-scores (fractal dimension +1SD: $b = -0.10$; 95% CI -0.18 to -0.02) after adjusting for age, sex, educational level, and reading ability. This association lost statistical significance after additional adjustment for total WMH volume (fractal dimension +1SD: $b = -0.16$; 95% CI -0.36–0.03; $p = 0.10$). [Fig. 1](#) shows an example of WMH in two patients (A and B) with similar WMH volume (A = 11.4 mL; B = 12.2 mL), but a more than 2 standard deviation difference in concavity index (concavity index Z-score: A = 1.06; B = 2.82). No associations were found between shape of deep WMH (i.e., eccentricity, fractal dimension) and cognitive functioning ([Table 3](#)).

We repeated the analyses for each vascular disease group separately ([Supplemental Table 2 and 3](#)). For memory function the results were fairly similar although the effect estimates varied somewhat across disease groups, but confidence intervals showed considerable overlap. This was also found for executive functioning, except for the AAA group where associations with periventricular/confluent WMH shape features were stronger, although it should be noted that this group was rather small.

4. Discussion

In this large cohort study among patients with a history of vascular disease, a larger total WMH volume was associated with decreased executive functioning, but not with memory performance. A more complex shape of periventricular/confluent WMH was associated with both decreased executive functioning and decreased memory performance. Furthermore, the association between WMH shape measured by the concavity index and executive functioning was independent of WMH volume. We did not find an association between deep WMH shape and cognitive functioning.

Only a few studies have been published on WMH shape analysis in CSVD ([de Bresser et al., 2018](#); [Ghaznawi et al., 2019](#); [Gwo et al., 2019](#); [Kant et al., 2019](#); [Lange et al., 2017](#)). To the best of our knowledge, only one study has examined the relationship between WMH shape and cognitive functioning ([Lange et al., 2017](#)). This study found that in two heterogeneous samples largely consisting of patients with cognitive impairment of various etiologies (e.g., Alzheimer's disease, vascular dementia, mixed-type), a more irregular shape of WMH (expressed by the "confluency sum score") was associated with a decrease in mental speed, executive functioning and mini-mental state examination performance ([Lange et al., 2017](#)). Notably, these associations were also independent of WMH volume, which is in agreement with our findings. Additionally, our study shows that this association already exists in persons with preclinical cognitive decline. We also show that within this population the association more specifically pertains to periventricular/confluent WMH and not too deep WMH, whereas [Lange et al.](#) examined shape of WMHs as a whole.

A wide variety of shape features and shape analysis methods exist ([Ghaznawi et al., 2019](#); [Gwo et al., 2019](#); [Lange et al., 2017](#); [Li and Tavares, 2014](#)). Because WMH shape analysis in CSVD is a new area of research, it is unclear which shape features best capture the relevant shape variation of WMH. [Gwo et al.](#) examined the applicability of Zernike polynomials of WMH lesions, which describe both lower order features such as gross shape and global contour and higher order features such as fine topological details ([Gwo et al., 2019](#); [Gwo and Wei, 2016](#)). Although they were able to

Table 3
Association between WMH volume, shape and cognitive functioning

	Model	Memory (Z-score), <i>b</i> (95% CI)	Executive functioning (Z-score), <i>b</i> (95% CI)
Total WMH volume (Z-score) ^a	1	-0.08 (-0.16 – 0.00)	-0.09 (-0.17 – -0.01)*
Periventricular/confluent WMH shape features (Z-scores) ^b			
Solidity, per -1 SD	1	-0.08 (-0.16 – 0.00)	-0.09 (-0.20 – -0.02)*
	2	-0.04 (-0.17 – 0.09)	-0.07 (-0.20 – 0.06)
Convexity, per -1 SD	1	0.02 (-0.05 – 0.09)	-0.02 (-0.09 – 0.05)
	2	0.00 (-0.07 – 0.08)	-0.04 (-0.12 – 0.03)
Concavity index, per +1 SD	1	-0.06 (-0.13 – 0.02)	-0.13 (-0.20 – -0.06)***
	2	-0.04 (-0.12 – 0.04)	-0.12 (-0.19 – -0.04)**
Fractal dimension, per +1 SD	1	-0.10 (-0.18 – -0.02)*	-0.06 (-0.14 – 0.01)
	2	-0.16 (-0.36 – 0.03)	0.07 (-0.12 – 0.25)
Deep WMH shape features (Z-scores) ^{b,c}			
Eccentricity, per +1 SD	1	0.07 (-0.02 – 0.16)	0.03 (-0.06 – 0.13)
	2	0.07 (-0.03 – 0.16)	0.02 (-0.07 – 0.11)
Fractal dimension, per +1 SD	1	0.05 (-0.05 – 0.15)	0.04 (-0.06 – 0.13)
	2	0.05 (-0.04 – 0.15)	0.04 (-0.05 – 0.14)

b values are unstandardized linear regression coefficients with 95% confidence intervals.

Model 1: adjusted for age, sex, educational level, and reading ability. Model 2: model 1 with additional adjustment for natural log-transformed total WMH volume (%ICV).

Key: %ICV, percentage of intracranial volume; SD, standard deviation; WMH, white matter hyperintensities.

^a Natural log-transformed total WMH volume (%ICV).

^b the +1 or -1 change in standard deviation denotes the direction of increasing shape complexity. For example, lower solidity and higher concavity both indicate increasing shape complexity.

^c Analysis performed only in patients with deep WMH lesions (*n* = 340).

* *p* ≤ 0.05;

** *p* ≤ 0.01;

*** *p* ≤ 0.001.

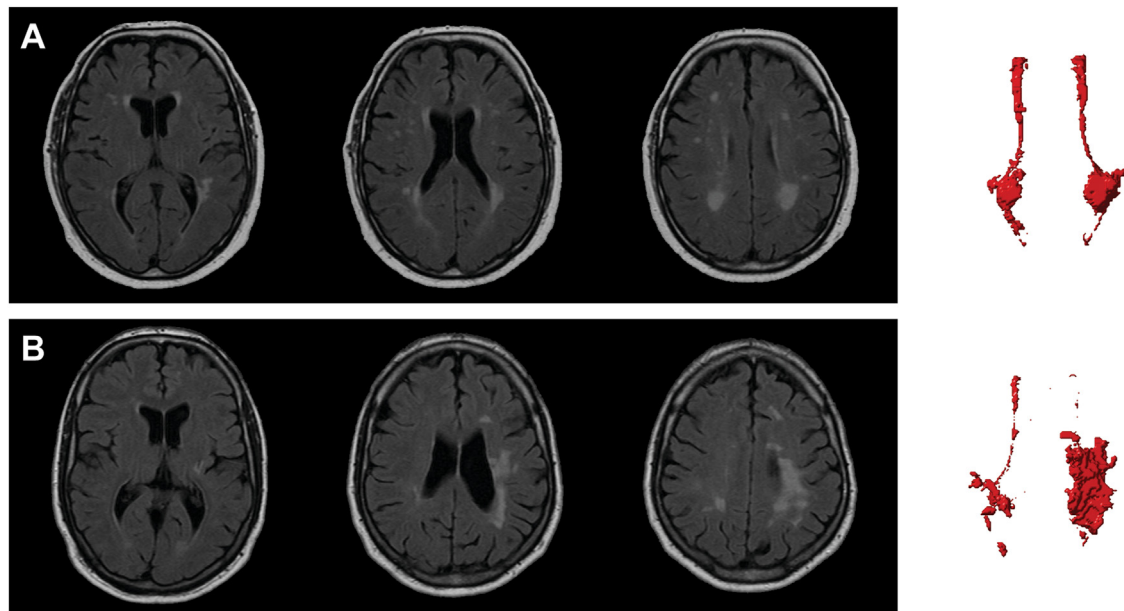


Fig. 1. Example of WMH shape difference in two patients (A, B) with comparable WMH volume (11.4 mL vs. 12.2 mL, respectively) but a 2.7 SD difference (Z-scores: 0.10 vs. 2.82, respectively) in concavity index. The 3 leftmost images in each row are axial FLAIR images at three different levels. The rightmost image is a top-down view of a volumetric rendering of the periventricular/confluent WMH segmentation. Note, the more complex shape of the periventricular/confluent WMH in the patient with the highest concavity index (B). For interpretation of the references to color in this figure legend, the reader is referred to the Web version of this article.

quantify shape, and cluster WMH lesions into distinctive groups, associations with determinants and outcomes were not assessed. We previously performed a broad exploration of available shape features to determine the most optimal features that capture the possible variations in WMH shape best (de Bresser et al., 2018; Ghaznawi et al., 2019). However, examining the relation of these features with determinants and outcomes is also important to determine which variations in shape of WMHs are clinically relevant.

Meta-analyses have shown that WMHs have a small and global detrimental effect on cognitive functioning (Debette and Markus, 2010; Kloppenborg et al., 2014). We found an association between WMH volume and executive functioning and memory, although the latter was not statistically significant. For WMH shape, we found that concavity index was associated with executive functioning but not with memory, and fractal dimension was associated with memory but not executive functioning. An hypothetical

explanation for this, is that WMH shape is not only related to the underlying pathology of WMHs, but also to their etiology, and different small vessel etiologies are known to have different effects on cognitive functioning.

Several mechanisms have been suggested for the relation between WMHs and cognitive functioning, all of which revolve around disruption of brain pathways (Prins and Scheltens, 2015). However, the extent of disruption for different underlying pathological changes (e.g., non-ischemic changes to necrosis) can vary (Gouw et al., 2011), which might explain the variable relationship of WMH volume with cognitive functioning in previous studies (Debette and Markus, 2010; Kloppenborg et al., 2014). Shape irregularity and confluency of WMH have been linked to the severity of WMH pathology (Fazekas et al., 1998; Gouw et al., 2011). This suggests that WMH shape may be a better determinant of cognitive functioning, compared to WMH volume. Our results seem to give support to this hypothesis, since the association between WMH shape (measured by concavity index) and cognitive functioning was independent of WMH volume. We think there are 2 likely explanations for this which partially overlap: WMH shape correlates with differences in etiology and/or pathological severity, which in turn differentially relate to cognitive functioning. As mentioned previously, this has been shown in periventricular WMH, where irregular (complex) shape is related to ischemia and more severe tissue damage, and smooth “caps and bands” to non-ischemic causes and more benign tissue changes (Fazekas et al., 1998). The exact mechanisms which lead to complex shape remain to be researched. However, a general observation of human pathophysiology suggests that – in general – benign processes are often controlled whereas less benign processes show loss of control and develop more irregular boundaries (e.g., neoplasms). The same may hold true for WMH pathophysiology.

Strengths of our study are the large size of the cohort, the semi-automatic WMH segmentation and automated image processing techniques to determine WMH shape features automatically, and the examination of two cognitive domains. Furthermore, the adjustment of our analyses for WMH volume allowed us to estimate if the association of WMH shape with cognitive functioning was independent of WMH volume. Moreover, the use of neuropsychological tests that are sensitive to mild impairments in cognitive functioning and the available data on premorbid cognitive functioning allowed detection of more subtle associations.

A limitation is that all participants had one or more vascular diseases, which might limit generalizability of our results to the general population. However, vascular disease is linked to the development of WMH and therefore these findings are especially of interest to this population. Another limitation is the use of 2-dimensional FLAIR MRI images with anisotropic voxels, which could have resulted in a less accurate approximation of WMH shape compared to the use of 3-dimensional FLAIR images with isotropic voxel size. However, even with use of these 2-dimensional FLAIR MRI images we were able to find relevant associations with WMH shape. Lastly, values of fractal dimension were very low. On 3-dimensional data values between 2 and 3 are expected whereas in our data the 90th percentile was already below 2. A likely explanation is that the implementation of box-counting that we use is suboptimal for WMH morphology and is better fitted for cubic shapes. Nonetheless, FD did differ between WMH lesions and showed a relation with cognitive functioning before WMH volume correction, suggesting that some relevant information about WMH lesions is captured.

Our findings are relevant because they suggest that WMH shape may be a new method to characterize the impact of WMHs on cognitive function. WMHs are highly prevalent in the older population, but their effect size on cognitive functioning is small, possibly

because conventional methods (e.g., volumetry, Fazekas score) do not correlate with the severity of underlying pathology. New methods to better characterize WMHs, for example, with shape features, will help in the study of risk factors and differential cognitive outcomes of WMHs.

In conclusion, WMH shape is associated with cognitive functioning in patients with vascular disease. Our results suggest that WMH shape contains additional information about WMH burden, not otherwise captured by WMH volume.

Disclosure statement

The authors report no conflict of interest.

Acknowledgements

The research of Jeroen Hendrikse has received funding from the European Research Council under the European Union's Horizon 2020 Programme (H2020) / ERC grant agreement no. 637024 (HEARTOFSTROKE) and H2020 grant agreement No 666881, SVDs@target. Jeroen Hendrikse is supported by the Netherlands Organization for Scientific Research (NWO) under grant no. 91712322. The research of Jeroen de Bresser is supported by Alzheimer Nederland under grant WE.03-2019-08. We thank all the members of the Utrecht Cardiovascular Cohort-Second Manifestations of Arterial disease-Studygroup (UCC-SMART Study Group): F.W. Asselbergs and H.M. Nathoe, Department of Cardiology; G.J. de Borst, Department of Vascular Surgery; M.L. Bots and M.I. Geerlings, Julius Center for health Sciences and Primary Care; M.H. Emmelot, Department of Geriatrics; P.A. de Jong and T. Leiner, Department of Radiology; A.T. Lely, Department of Obstetrics & Gynecology; N.P. van der Kaaij, Department of Cardiothoracic Surgery; L.J. Kappelle and Y.M. Ruijgrok, Department of Neurology; M.C. Verhaar, Department of Nephrology, F.L.J. Visseren (chair) and J. Westerink, Department of Vascular Medicine, University Medical Center Utrecht and Utrecht University.

Furthermore, we would like to thank Jasmin Keller for her work on data acquisition and reproducibility testing.

CRediT authorship contribution statement

Maarten H.T. Zwartbol: Writing – original draft, Conceptualization, Methodology, Formal analysis, Investigation. **Rashid Ghaznawi:** Data curation, Investigation. **Myriam Jaarsma-Coes:** Data curation, Software. **Hugo Kuijff:** Data curation, Writing – review & editing, Software. **Jeroen Hendrikse:** Funding acquisition, Supervision. **Jeroen de Bresser:** Funding acquisition, Supervision, Writing – review & editing, Conceptualization, Methodology. **Mirjam I. Geerlings:** Project administration, Supervision, Writing – review & editing, Resources, Conceptualization, Formal analysis.

Supplementary materials

Supplementary material associated with this article can be found, in the online version, at doi:[10.1016/j.neurobiolaging.2022.08.009](https://doi.org/10.1016/j.neurobiolaging.2022.08.009).

References

- Anbeek, P., Vincken, K.L., van Osch, M.J., Bisschops, R.H., van der Grond, J., 2004. Probabilistic segmentation of white matter lesions in MR imaging. *Neuroimage*. 21, 1037–1044. doi:[10.1016/j.neuroimage.2003.10.012](https://doi.org/10.1016/j.neuroimage.2003.10.012).
- Brand, N., Jolles, J., 1985. Learning and retrieval rate of words presented auditorily and visually. *J. Gen. Psychol.* 112, 201–210. doi:[10.1080/00221309.1985.9711004](https://doi.org/10.1080/00221309.1985.9711004).
- Burgess, P.W., Shallice, T., 1996. Bizarre responses, rule detection and frontal lobe lesions. *Cortex*. 32, 241–259. doi:[10.1016/S0010-9452\(96\)80049-9](https://doi.org/10.1016/S0010-9452(96)80049-9).

- de Bresser, J., Kuijff, H.J., Zaanen, K., Viergeever, M.A., Hendrikse, J., Biessels, G.J., Algra, A., Van Den Berg, E., Bouvy, W., Brundel, M., Heringa, S., Kappelle, L.J., Leemans, A., Luijten, P.R., Mali, W.P.T.M., Rutten, G.E.H.M., Vincken, K.L., Zwanenburg, J., 2018. White matter hyperintensity shape and location feature analysis on brain MRI; Proof of principle study in patients with diabetes. *Sci. Rep.* 8, 1–10. doi:10.1038/s41598-018-20084-y.
- Debette, S., Markus, H.S., 2010. The clinical importance of white matter hyperintensities on brain magnetic resonance imaging: systematic review and meta-analysis. *BMJ* 341. doi:10.1136/bmj.c3666, c3666–c3666.
- Esteban, F.J., Sepulcre, J., de Miras, J.R., Navas, J., de Mendizábal, N.V., Goñi, J., Quesada, J.M., Bejarano, B., Villoslada, P., 2009. Fractal dimension analysis of grey matter in multiple sclerosis. *J. Neurol. Sci.* 282, 67–71. doi:10.1016/j.jns.2008.12.023.
- Fazekas, F., Schmidt, R., Scheltens, P., 1998. Pathophysiologic mechanisms in the development of age-related white matter changes of the brain, in: *Dementia and Geriatric Cognitive Disorders*. doi:10.1159/000051182.
- Geerlings, M.I., Appelman, A.P., Vincken, K.L., Algra, A., Witkamp, T.D., Mali, W.P., van der Graaf, Y., Group, S.S., 2010. Brain volumes and cerebrovascular lesions on MRI in patients with atherosclerotic disease. The SMART-MR study. *Atherosclerosis* 210, 130–136. doi:10.1016/j.atherosclerosis.2009.10.039.
- Ghaznawi, R., Geerlings, M.I., Jaarsma-Coes, M.G., Zwartbol, M.H.T., Kuijff, H.J., van der Graaf, Y., Witkamp, T.D., Hendrikse, J., de Bresser, J., 2019. The association between lacunes and white matter hyperintensity features on MRI: The SMART-MR study. *J. Cereb. Blood Flow Metab.* 39, 2486–2496. doi:10.1177/0271678X18800463.
- Gouw, A.A., Seewann, A., van der Flier, W.M., Barkhof, F., Rozemuller, A.M., Scheltens, P., Geurts, J.J.G.G., 2011. Heterogeneity of small vessel disease: a systematic review of MRI and histopathologic correlations. *J. Neurol. Neurosurg. Psychiatry* 82, 126–135. doi:10.1136/jnnp.2009.204685.
- Gwo, C.-Y., Zhu, D.C., Zhang, R., 2019. Brain white matter hyperintensity lesion characterization in T2 fluid-attenuated inversion recovery magnetic resonance images: shape, texture, and potential growth. *Front. Neurosci.* 13, 1–15. doi:10.3389/fnins.2019.00353.
- Gwo, C.Y., Wei, C.H., 2016. Shoeprint retrieval: core point alignment for pattern comparison. *Sci. Justice*. doi:10.1016/j.scijus.2016.06.004.
- Kant, I.M.J., Mutsaerts, H.J.M.M., van Montfort, S.J.T., Jaarsma-Coes, M.G., Witkamp, T.D., Winterer, G., Spies, C.D., Hendrikse, J., Slooter, A.J.C., de Bresser, J., Armbruster, F.P., Böcher, A., Boraschi, D., Borchers, F., Della Camera, G., van Dellen, E., Diehl, I., Dschietzig, T.B., Feinkohl, I., Fillmer, A., Gallinat, J., Hafen, B., Hartmann, K., Heidtke, K., Helmschrodt, A., Italiani, P., Ittermann, B., Krause, R., Kronabel, M., Kühn, S., Lachmann, G., Melillo, D., Menon, D.K., Moreno-López, L., Mörgeli, R., Nürnberg, P., Ofosu, K., Olbert, M., Pietzsch, M., Pischon, T., Preller, J., Ruppert, J., Schneider, R., Stamatakis, E.A., Weber, S., Weyer, M., Winzeck, S., Wolf, A., Yürek, F., Zacharias, N., 2019. The association between frailty and MRI features of cerebral small vessel disease. *Sci. Rep.* 9, 1–9. doi:10.1038/s41598-019-47731-2.
- Kempton, M.J., Underwood, T.S.A., Brunton, S., Stylios, F., Ettinger, U., Smith, M.S., Lovestone, S., Crum, W.R., 2013. A comprehensive testing protocol for MRI neuroanatomical segmentation techniques: Evaluation of a novel lateral ventricle segmentation method. *58*, 1051–1059. doi:10.1016/j.neuroimage.2011.06.080.A.
- Kloppenborg, R.P., Nederkoorn, P.J., Geerlings, M.I., van den Berg, E., 2014. Presence and progression of white matter hyperintensities and cognition: a meta-analysis. *Neurology* 82, 2127–2138. doi:10.1212/wnl.0000000000000505.
- Lange, C., Suppa, P., Mäurer, A., Ritter, K., Pietrzyk, U., Steinhagen-Thiessen, E., Fiebach, J.B., Spies, L., Buchert, R., 2017. Mental speed is associated with the shape irregularity of white matter MRI hyperintensity load. *Brain Imaging Behav* 11, 1720–1730. doi:10.1007/s11682-016-9647-x.
- Li, S., Tavares, J.M.R.S., 2014. *Shape Analysis in Medical Image Analysis*. Springer International Publishing, Switzerland.
- Liu, E.J., Cashman, K.V., Rust, A.C., 2015. Optimising shape analysis to quantify volcanic ash morphology. *GeoResJ* 8, 14–30. doi:10.1016/j.grj.2015.09.001.
- Loizou, C.P., Petroudi, S., Seimenis, I., Pantziaris, M., Pattichis, C.S., 2015. Quantitative texture analysis of brain white matter lesions derived from T2-weighted MR images in MS patients with clinically isolated syndrome. *J. Neuroradiol.* 42, 99–114. doi:10.1016/j.neurad.2014.05.006.
- Moisy, F., 2008. boxcount [WWW Document]. MathWorks File Exch. URL <https://www.mathworks.com/matlabcentral/fileexchange/13063-boxcount>. Accessed 2nd of May 2020.
- Muller, M., Appelman, A.P., van der Graaf, Y., Vincken, K.L., Mali, W.P., Geerlings, M.I., 2011. Brain atrophy and cognition: interaction with cerebrovascular pathology? *Neurobiol. Aging* 32, 885–893. doi:10.1016/j.neurobiolaging.2009.05.005.
- Murphy, K., van Ginneken, B., Schilham, A.M.R., de Hoop, B.J., Gietema, H.A., Prokop, M., 2009. A large-scale evaluation of automatic pulmonary nodule detection in chest CT using local image features and k-nearest-neighbour classification. *Med. Image Anal.* 13, 757–770. doi:10.1016/j.media.2009.07.001.
- Osterrieth, P., 1944. Filetest de copie d'une figure complex: contribution a l'etude de la perception et de la memoire [The test of copying a complex figure: a contribution to the study of perception and memory]. *Arch. Psychol.* 30, 286–356.
- Pantoni, L., 2010. Cerebral small vessel disease: from pathogenesis and clinical characteristics to therapeutic challenges. *Lancet Neurol* 9, 689–701. doi:10.1016/S1474-4422(10)70104-6.
- Prins, N.D., Scheltens, P., 2015. White matter hyperintensities, cognitive impairment and dementia: an update. *Nat. Rev. Neurol.* 11, 157–165. doi:10.1038/nrneuro.2015.10.
- Robertson, I.H., Ward, T., Ridgeway, V., Nimmo-Smith, I., 1996. The structure of normal human attention: The Test of Everyday Attention. *J. Int. Neuropsychol. Soc.* 2, 525–534.
- Schmand, B., Geerlings, M.I., Jonker, C., Lindeboom, J., 1998. Reading ability as an estimator of premorbid intelligence: does it remain stable in emergent dementia? *J. Clin. Exp. Neuropsychol.* 20, 42–51. doi:10.1076/jcen.20.1.42.1485.
- Vogels, R.L., Oosterman, J.M., van Harten, B., Gouw, A.A., Schroeder-Tanka, J.M., Scheltens, P., van der Flier, W.M., Weinstein, H.C., 2007. Neuroimaging and correlates of cognitive function among patients with heart failure. *Dement. Geriatr. Cogn. Disord.* 24, 418–423. doi:10.1159/000109811.
- Wardlaw, J.M., Smith, E.E., Biessels, G.J., Cordonnier, C., Fazekas, F., Frayne, R., Lindley, R.L., O'Brien, J.T., Barkhof, F., Benavente, O.R., Black, S.E., Brayne, C., Breteler, M., Chabriat, H., DeCarli, C., de Leeuw, F.-E.E., Doubal, F., Dering, M., Fox, N.C., Greenberg, S., Hachinski, V., Kilimann, I., Mok, V., van Oostenbrugge, R., Pantoni, L., Speck, O., Stephan, B.C.M.M., Teipel, S., Viswanathan, A., Werring, D., Chen, C., Smith, C., van Buchem, M., Norrving, B., Gorelick, P.B., Dichgans, M., Changes, St.R.V., O, J.T., Barkhof, F., Benavente, O.R., Black, S.E., Brayne, C., Breteler, M., Chabriat, H., DeCarli, C., de Leeuw, F.-E.E., Doubal, F., Dering, M., Fox, N.C., Greenberg, S., Hachinski, V., Kilimann, I., Mok, V., van Oostenbrugge, R., Pantoni, L., Speck, O., M Stephan, B.C., Teipel, S., Viswanathan, A., Werring, D., Chen, C., Smith, C., van Buchem, M., Norrving, B., Gorelick, P.B., Dichgans, M., Oostenbrugge, R.van, Pantoni, L., Speck, O., Stephan, B.C.M.M., Teipel, S., Viswanathan, A., Werring, D., Chen, C., Smith, C., van Buchem, M., Norrving, B., Gorelick, P.B., Dichgans, M., Oostenbrugge, R.van, Pantoni, L., Speck, O., Stephan, B.C.M.M., Teipel, S., Viswanathan, A., Werring, D., Chen, C., Smith, C., van Buchem, M., Norrving, B., Gorelick, P.B., Dichgans, M., 2013. Neuroimaging standards for research into small vessel disease and its contribution to ageing and neurodegeneration. *Lancet Neurol* 12, 822–838. doi:10.1016/S1474-4422(13)70124-8.
- Wilkins, A.J., Shallice, T., McCarthy, R., 1987. Frontal lesions and sustained attention. *Neuropsychologia* 25, 359–365. doi:10.1016/0028-3932(87)90024-8.
- Zhang, L., Liu, J.Z., Dean, D., Sahgal, V., Yue, G.H., 2006. A three-dimensional fractal analysis method for quantifying white matter structure in human brain. *J. Neurosci. Methods* 150, 242–253. doi:10.1016/j.jneumeth.2005.06.021.